

USING AN ELECTROSTATIC ACCELERATOR TO DETERMINE
THE
STEREOCHEMICAL STRUCTURES OF MOLECULAR IONS

MASTER

by

Donald S. Gemmell

Prepared for
Sixth Conference
on the
Applications of Accelerators in Research and Industry
Denton, Texas
November 3-5, 1980

DISCLAIMER

This document contains information which was prepared by an agency of the United States Government. Neither the United States Government nor any agency thereof makes any warranty, expressed or implied, or assumes any legal liability or responsibility for the accuracy, completeness, or usefulness of the information contained herein, or for the results obtained from the use of the information. It is advised that individuals and organizations should obtain and verify the accuracy of this information by independent means. This document is intended to provide a basis for the development of appropriate standards and procedures for the use of this information. It is not intended to be used as a basis for the development of any agency's internal compliance systems. The United States Government is not responsible for any errors or for any consequences arising from the use of the information contained herein.



ARGONNE NATIONAL LABORATORY, ARGONNE, ILLINOIS

**Operated under Contract W-31-109-Eng-38 for the
U. S. DEPARTMENT OF ENERGY**

REPRODUCTION OF THIS DOCUMENT IS UNLIMITED

DMS

USING AN ELECTROSTATIC ACCELERATOR TO DETERMINE THE STEREOCHEMICAL STRUCTURES OF MOLECULAR IONS

Donald S. Gemmell

Physics Division, D203, Argonne National Laboratory, Argonne, IL 60439

Summary

Traditional experimental techniques (e.g. studies on photon absorption or emission) for determining the stereochemical structures of neutral molecules are extremely difficult to apply to molecular ions because of problems in obtaining a sufficient spatial density of the ions to be studied. Recent high-resolution measurements on the energy and angle distributions of the fragments produced when fast (MeV) molecular-ion beams from an electrostatic accelerator dissociate ("Coulomb explode") in thin foils and in gases, offer promising possibilities for deducing the stereochemical structures of the molecular ions constituting the incident beams. Bond lengths have been determined in this way for several diatomic projectiles (H_2^+ , HeH^+ , CH^+ , NH^+ , OH^+ , N_2^+ , O_2^+ , etc.) with an accuracy of $\sim 0.01 \text{ \AA}$. H_3^+ has been demonstrated (for the first time) to be equilateral triangular and the interproton distance measured. Measurements on single fragments from CO_2^+ , N_2O^+ , $C_3H_3^+$, and CH_n^+ have revealed the gross structures of the projectiles. An apparatus has recently been constructed at Argonne to permit precise measurements on fragments in coincidence. The apparatus has been tested on a known structure (OH_2^+). The O-H bond length was found to be $1.0 \pm 0.04 \text{ \AA}$ and the H-O-H bond angle was measured as $110 \pm 2^\circ$. These values are in excellent agreement with those found in optical experiments (0.999 \AA and 110.5°). This "Coulomb explosion" technique can be expected to be refined in accuracy and to be extended to a wide range of molecular ions whose structures are inaccessible by other means.

Introduction

For the past couple of years at Argonne, high-resolution studies have been made on the foil- and gas-induced dissociation of fast molecular-ion beams produced by the 4-MV Dynamitron accelerator in Physics Division.¹⁻⁵ The measurements involve detection of dissociation fragments with a relative energy resolution of $\pm 3 \times 10^{-4}$ and an angular resolution of $\pm 1.5 \times 10^{-4}$ radians. Magnetically analyzed and tightly collimated molecular-ion beams are directed into a chamber (Fig. 1) containing the target foil (usually $\sim 100\text{-\AA}$ thick carbon) or gas. Sets of electrostatic deflector plates are located in the chamber both

upstream and downstream from the target. Charged fragments emerging from the target are directed into a 1-mm entrance aperture preceding an electrostatic analyzer located several meters downstream. Figure 2 shows a typical "ring pattern" obtained for a given fragment species.

The radius of such a pattern is proportional to the CM velocity acquired by these fragments primarily as a result of the "Coulomb explosions" initiated when the molecular projectiles are stripped of their binding electrons upon entering a foil target. For diatomic projectiles this CM velocity is proportional to the geometric mean of the two fragment-ion charge states and inversely proportional to the square root of their initial internuclear separation. The charge states inside the foil are the effective ionic charges that determine the stopping power. Outside the foil there is a distribution of (integral) charge states that can be experimentally determined. A knowledge of these charge states together with a measurement of the radial distribution of the intensity in a ring pattern (or along any radius of the ring) thus permits determination of the distribution of initial internuclear separations in the molecular-ion projectiles. (The non-uniform intensity distribution around the circumference of a ring pattern such as that in Fig. 2 is explained in terms of polarization "wake" effects².)

Measurements at Argonne using a wide range of diatomic projectiles (e.g. H_2^+ , HeH^+ , CH^+ , NH^+ , OH^+ , N_2^+ , O_2^+ , etc.) have shown that the projectile bond lengths may be determined to an accuracy of about 0.01 \AA with these techniques. In view of the extreme difficulties encountered in the "standard" experimental methods of determining the geometrical structures of molecular ions (it is hard to get a sufficient column density of the ions for the usual photon absorption or emission techniques), we have recently begun exploring the possibilities that our apparatus offers for structure determinations via the "Coulomb explosion" of fast polyatomic molecular-ion projectiles.⁶⁻¹¹ Related experiments are under way at the Weizmann Institute¹² and at Brookhaven National Laboratory.¹³

In the following we list some of the structure measurements that have been performed at Argonne. They fall into two categories: a) measurements on single

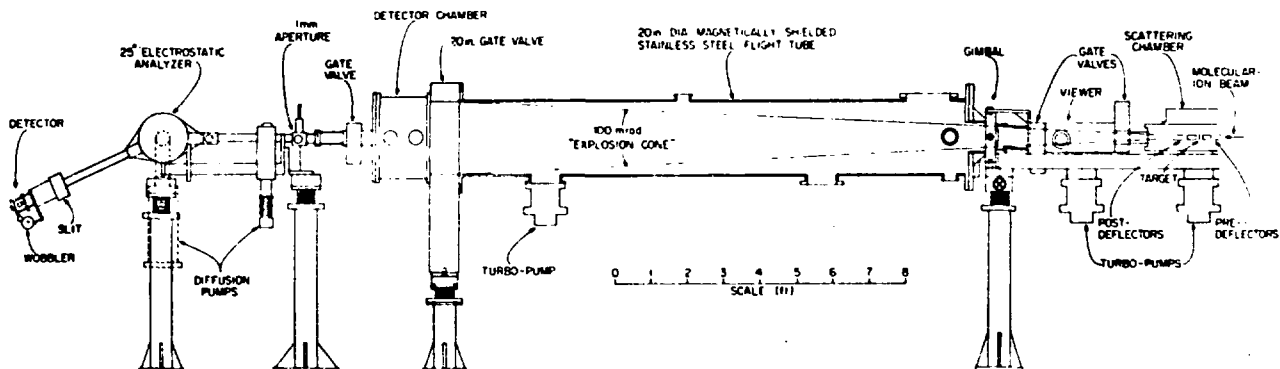


Fig. 1. Schematic diagram of the experimental arrangement at Argonne's 4-MV Dynamitron accelerator.

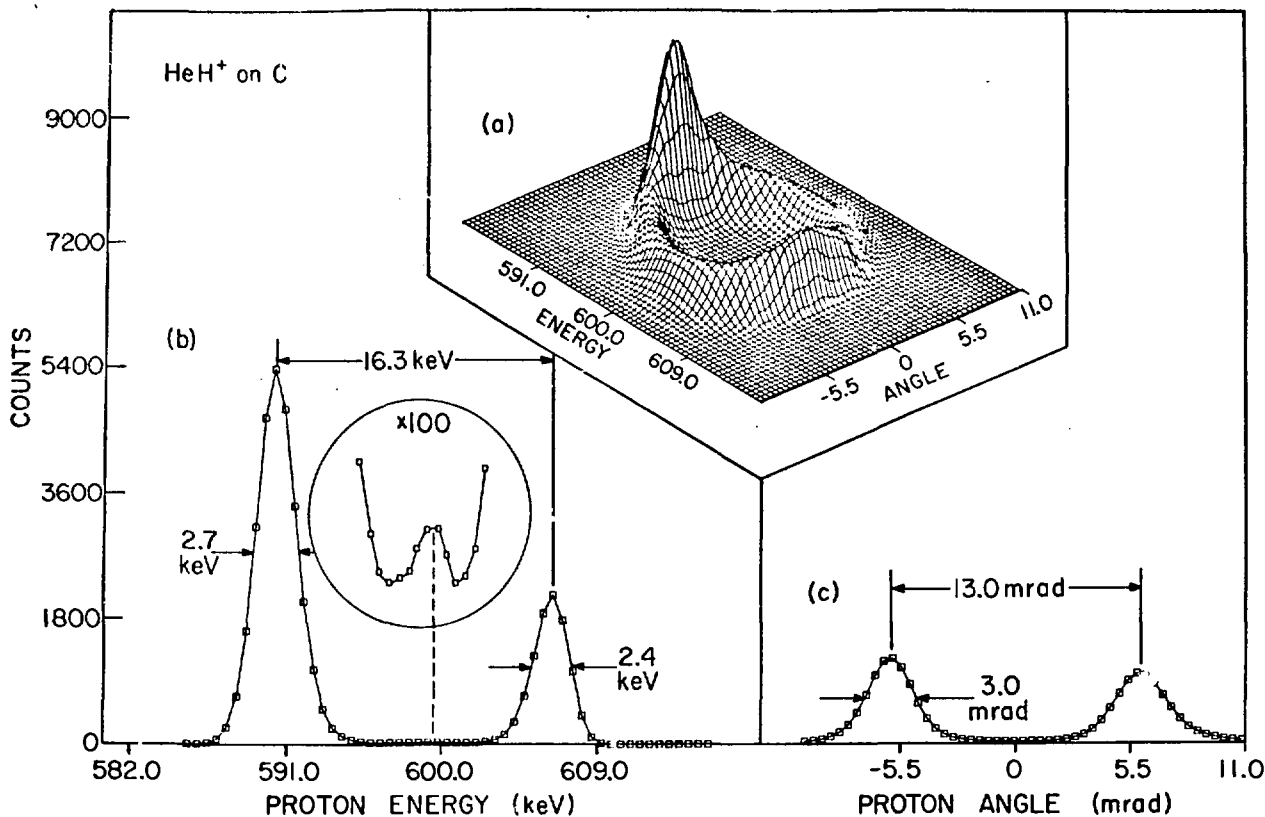


Fig. 2. "Ring pattern" for protons from 3.0-MeV HeH^+ dissociating in a 195-Å thick carbon foil (Ref. 2).

fragments and b) measurements in which two or more fragments from individual molecular-ion projectiles are detected in coincidence. Measurements on single-fragment distributions can be performed rapidly (typically a few minutes) and readily yield gross features of the projectile's structure. Thus, for example, our measurements on C^{2+} fragments from 3.6-MeV C_3H_3^+ ions dissociating in thin foils demonstrate that the carbons sit on the corners of an approximately equilateral triangle. [That is, we have a beam of cyclopropenyl ions and not propargyl ions (which are linear in carbons).] Similarly, our measurements on single fragments from OH_2^+ show that the protons are equivalent and that the oxygen is "in the middle". The accuracy in determining the bond length and bond angle in this case is modest because there are fairly wide ranges of values for these parameters that combine to give about the same Coulomb explosion velocity for any given fragment.

A difficulty associated with this type of measurement for polyatomic molecular ions lies in analyzing the effects of vibrational excitations of the projectiles. Excitations of some modes (e.g. symmetric breathing modes) can often be expected to result only in apparent changes in the bond lengths determined by the Coulomb-explosion method. However, many non-symmetric modes can result in apparent structures that differ markedly from the structure of the vibrationless ground state. It is therefore important to analyze the Coulomb-explosion data in terms of the specific modes that can be excited for each projectile species considered. The analysis can be greatly simplified if the projectiles can be prepared in their ground (or at most a small range of low-lying) vibrational states.

Polyatomic structures can be much more precisely determined if spatial and temporal coincidences are recorded for two or more dissociation fragments from a given projectile. With this in mind, we recently revised the apparatus at Argonne so as to permit a wide variety of coincidence measurements. We are now able to measure double or triple coincidences and record simultaneously information on fragment charge states, energies, and flight times from the target. The system has been tested with various simple diatomic and triatomic projectiles (H_2^+ , HeH^+ , CH^+ , NH^+ , OH^+ , H_3^+ , CH_2^+ , NH_2^+ , OH_2^+ , etc.).

Measurements on Single Fragments from Polyatomic Projectiles

H_3^+ . A joint study⁶ of the simplest polyatomic molecular ion, H_3^+ , was undertaken at the University of Lyon, the Weizmann Institute and Argonne National Laboratory. Each laboratory performed a measurement based on the Coulomb explosion of fast H_3^+ ions. Although somewhat different techniques were used the three measurements gave results in agreement with one another. It was experimentally demonstrated (for the first time) that H_3^+ is equilateral triangular in shape. The three measurements of the proton-proton bond distance yielded 0.97 ± 0.03 Å (Argonne), 0.95 ± 0.06 Å (Lyon), and 1.1 ± 0.2 Å (Weizmann Institute). Figure 3 shows a comparison of these results with a recent calculation of Carney¹⁴ based on the vibrational-state population parameters of Smith and Futrell.¹⁵ (The vibrational ground state of H_3^+ has a calculated bond length of 0.91 Å.)

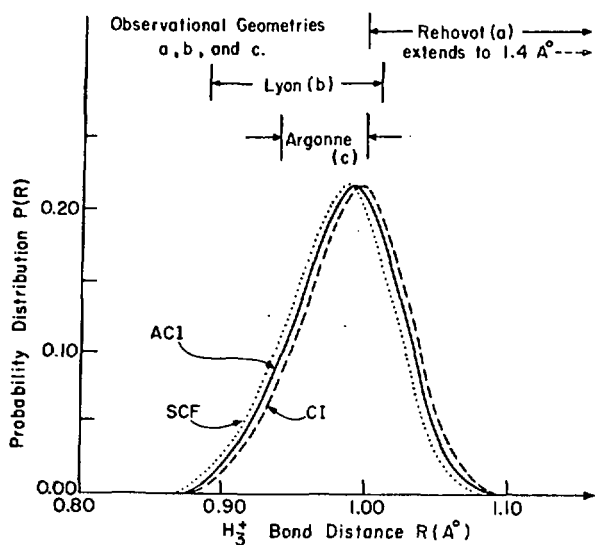


Fig. 3. Comparison between measured (Ref. 6) and calculated (Ref. 14) distributions in the proton-proton bond distance in H_3^+ (from Ref. 14).

CO_2^+ and N_2O^+ . A typical example of the manner in which gross structures may be rapidly determined by Coulomb explosion techniques is to be found in our recent studies with 3.5-MeV beams of CO_2^+ and N_2O^+ . These molecular ions in their ground and low-lying states are known¹⁶ to be linear; but while CO_2^+ has the symmetric form (O-C-O), N_2O^+ is asymmetric (N-N-O). Figure 4 shows $\theta = 0$ energy spectra for O^{4+} and C^{2+} from CO_2^+ and O^{4+} and N^{3+} from N_2O^+ . Similar spectra were obtained for fragments emerging in other charge states. The principal structural characteristics are evident from just a casual inspection of Fig. 4. The existence of only two peaks in Fig. 4(a) indicates that the two oxygen atoms in CO_2^+ are equivalent. The existence of just one peak in Fig. 4(b) shows that the carbon atom is central in a linear molecule (no net Coulomb-explosion velocity). The two peaks in Fig. 4(c) show that the oxygen atom in N_2O^+ lies "on the outside" and the three peaks in Fig. 4(d) show that one nitrogen atom is "on the outside" and that one is in the center of a linear molecule. The central peak in Fig. 4(d) is much more strongly populated than the two side peaks because many more incident orientations contribute to it.

From these considerations, it can be seen that by simply counting the number of peaks in each spectrum, one can infer that both CO_2^+ and N_2O^+ are linear with structures (O-C-O) and (N-N-O). To obtain precise values for the bond lengths and angles, a more detailed analysis is obviously required.

CH_n^+ ($n = 0, 4$). The proton and the carbon fragments arising from the Coulomb explosion of CH^+ , CH_2^+ , CH_3^+ and CH_4^+ have been studied at beam velocities corresponding to 0.194 MeV/a.m.u.¹⁰ In Fig. 5 we show the measured energy widths (FWHM) of outgoing C^{4+} ions that emerge after the incident beam strikes a foil target. The value of 6.1 keV for incident C^+ represents the contribution of energy straggling convoluted with both the beam energy spread and the resolving power of the electrostatic analyzer system. The Coulomb explosion of the highly asymmetric CH^+ ions adds a

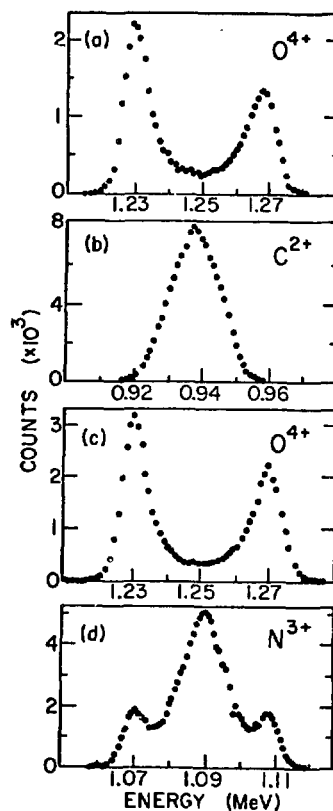


Fig. 4. Energy spectra at $\theta = 0$ for (a) O^{4+} and (b) C^{2+} resulting from 3.5-MeV CO_2^+ bombarding a 133-Å thick C foil, and for (c) O^{4+} and (d) N^{3+} resulting from 3.5-MeV N_2O^+ bombarding a 160-Å thick carbon foil (Ref. 7).

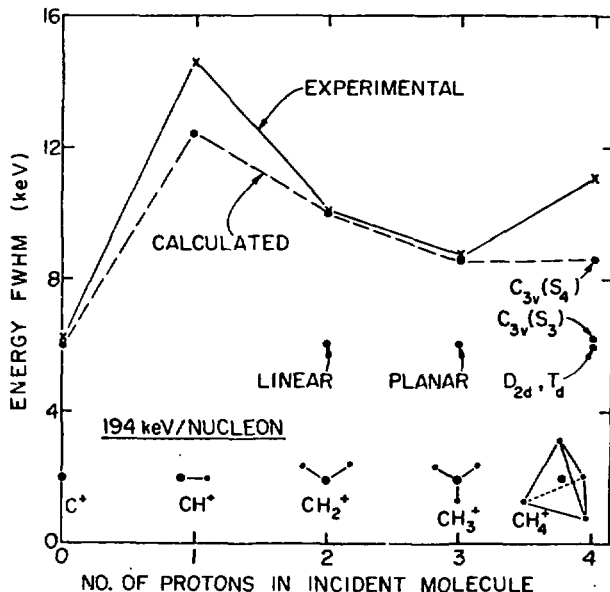


Fig. 5. Comparison of energy widths of C^{4+} spectra for $CH_n^+ + C^{4+}$. The calculations are based on a carbon-ion effective charge of 3.5 and neglect wake forces.¹⁰

large contribution which increases the measured width to 14.6 keV. For the more symmetric CH_2^+ ions, because of near cancellation of the impulses produced by each proton on the carbon ion, the Coulomb explosion is reduced and thus we measure a width of only 10.1 keV. If CH_2^+ were rigidly linear, the width would be expected to be close to the C^+ straggling value of 6.1 keV (the width would actually be somewhat greater than 6.1 keV because of charge-stage fluctuation effects that modify the Coulomb explosion while the ion fragments are within the target foil). A similar effect is seen in the measurement of the carbon width for the dissociation of CH_3^+ . Again, the width is increased over the minimum that one would expect for rigid planar structure; however, it is smaller than either of the CH^+ or CH_2^+ results. The data for CH_4^+ show a dramatic departure from this general trend. The measured width of 11.1 keV is larger than all but the CH^+ measurement. This indicates a highly asymmetric proton distribution around the carbon nucleus and is most likely a consequence of the Jahn-Teller distortion of CH_4^+ .

The dashed line in Fig. 5 shows the width calculated on the basis of a very crude model in which it is assumed that rigid structures having carbon charges of 3.5 and proton charges of 1.0 Coulomb explode. No attempt was made here to include the effects of molecular vibrations, wakes, multiple scattering, charge-state distributions, etc. These calculations thus serve only as a rough guide to the possible structures of the projectiles and are not to be interpreted as determining the actual structures. The calculation for CH^+ assumes a bond length of 1.13 Å. For CH_2^+ a carbon-proton distance of 1.03 Å is assumed and the H-C-H angle is taken to be 140° (a guess based on the expectation that the bond angle will be close to the value of 131° known¹⁶ for the isoelectronic molecule BH_2). For CH_3^+ the calculation assumes a rigid pyramidal structure with an inter-proton distance of 1.08 Å and with the carbon ion 0.2 Å off the proton plane. The values calculated for CH_4^+ were based on the four Jahn-Teller distorted structures derived by Dixon.¹⁷ As noted above, taking account of vibrational excitations of the projectiles can affect the implications of these calculations. For example, CH_3^+ is commonly thought to be planar¹⁶ and the results shown in Fig. 5 are consistent with a planar structure in which a low-frequency out-of-plane oscillation of the carbon ion exists with an amplitude of ~ 0.2 Å.

HCO^+ . In Table I we compare the diameters of the ring patterns obtained¹⁸ for C^{4+} , O^{3+} , and O^{5+} fragments from the foil-induced dissociation of HCO^+ and CO^+ of the same velocity (124 keV/nucleon). A cursory glance suffices to deduce that the triatomic beam ions must have the structure H-C-O and not C-O-H or C-H-O.

TABLE I

Diameters (in keV and mrad) of the ring patterns for C^{4+} , O^{3+} and O^{5+} fragments from the foil-induced dissociation of beams of 3.476-MeV CO^+ and 3.6-MeV HCO^+ .

Fragment	Diameter in keV		Diameter in mrad	
	CO^+	HCO^+	CO^+	HCO^+
C^{4+}	42.1	37.9	13.9	13.2
O^{3+}	37.6	39.1	8.8	9.2
O^{5+}	42.0	44.4	9.7	10.4

Coincidence Measurements

The beam line shown in Fig. 1 has been expanded to include a chamber containing movable detectors (Fig. 6) that permit coincidence measurements. The two detectors shown in Fig. 6 can be remotely positioned with an accuracy of about 0.001 in. anywhere on a 20-in. diameter circular area subtending an angle of 100 mrad at the target. The system has been calibrated with various diatomic beams and has recently been used to study H_3^+ (and its deuterated substitutions) and the ions CH_2^+ , NH_2^+ and OH_2^+ .

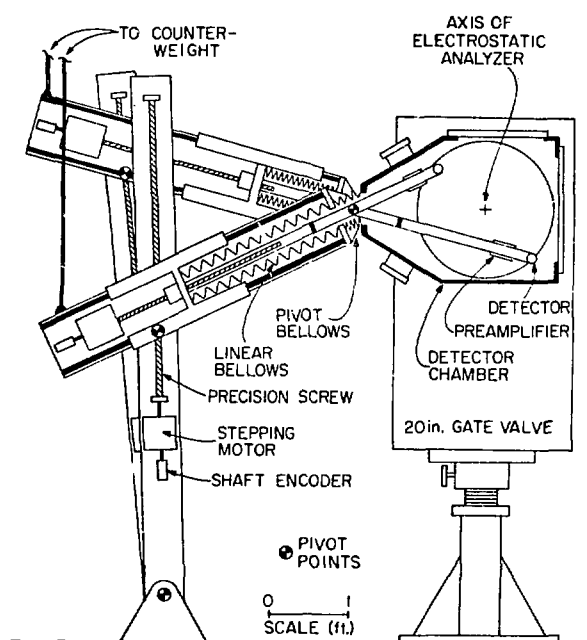


Fig. 6. Schematic diagram showing a cross-sectional view of the detector chamber and movable detector systems at Argonne's 4-MV Dyanmitron accelerator.

H_3^+ . Figure 7 shows the proton-proton coincidence counting rate obtained with a beam of 1.8-MeV H_3^+ striking a carbon foil.¹⁹ In these measurements one of the detected protons was counted in the electrostatic analyzer (ESA). The deflections and the ESA voltage were set so that the ESA detected "sideways-going" (in the C.M. frame) protons. The other detected proton was sensed in one of the movable semiconductor counters shown in Fig. 6. The abscissa in Fig. 7 is the angular separation of the two detected protons relative to the angular diameter of the proton ring pattern. For an equilateral triangular H_3^+ , one would expect the coincidence rate to peak at an abscissa value of 0.75. The slight upward shift in the experimental value (0.77) is explainable in terms of the decreased phase space available for larger angular separations.

CH_2^+ , NH_2^+ and OH_2^+ . Preliminary coincidence measurements have been performed for these dihydride ions.⁹ Of the three, only OH_2^+ has previously had its structure determined experimentally. From optical measurements Lew and Heiber²⁰ found the O-H bond length to be 0.999 Å and the H-O-H bond angle to be 110.5°.

Figure 8 shows a spatial scan of the proton-proton double coincidence rate for the foil-induced

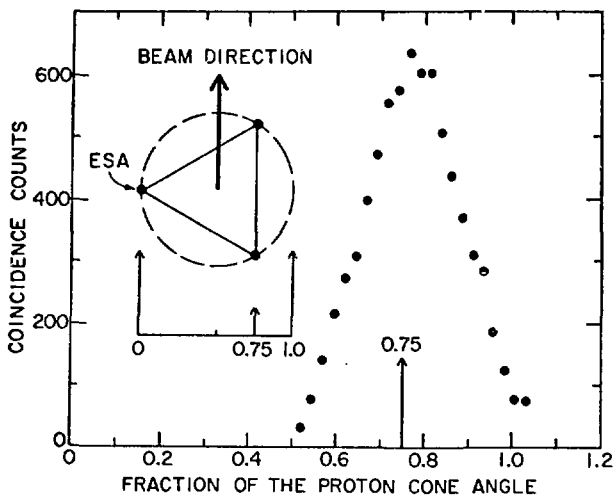


Fig. 7. Proton-proton counting rate as a function of the relative angular separation of the two detectors (the ESA and one of the movable detectors shown in Fig. 6) (Ref. 19). The protons arose from 1.8-MeV H_3^+ incident on a carbon foil 93-Å thick.

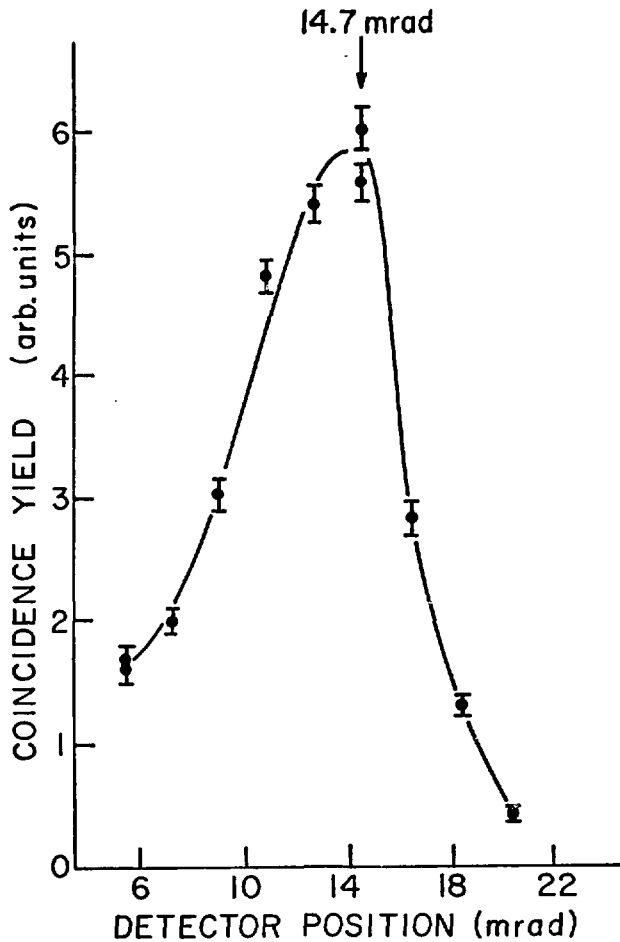


Fig. 8. Coincidence counting rate for protons from 3.6-MeV OH_2^+ dissociating in an 80-Å thick carbon foil (Ref. 9). The rate is plotted as a function of the angle between the electrostatic analyzer (set on the low-energy, $\theta = 0$ proton group) and one of the movable surface-barrier detectors (Fig. 6).

dissociation of 3.6-MeV OH_2^+ ions. Note that a given combination of post-deflector and ESA voltage settings amounts to choosing for study a limited subset of the incoming projectile orientations. For the data shown in Fig. 8, only those OH_2^+ ions in which one proton is trailing are selected. The angular radius of the proton ring pattern is 16.2 mrad. Thus the bond angle is close to $\beta = 180^\circ - \sin^{-1}(14.7/16.2) = 115^\circ$. Approximate corrections for the displaced CM and for the oxygen recoil result in values of $110 \pm 2^\circ$ and $1.0 \pm 0.04 \text{ \AA}$ for the bond angle and bond length, respectively. These values agree with those from the optical measurements.²⁰ Measurements with other orientations chosen in the ESA give similar results. A more detailed analysis, properly taking into account wake effects and multiple scattering, should result in a significant improvement in the level of accuracy.

Figure 9 shows a comparison of the results for foil-induced dissociation of 3.6-MeV CH_2^+ , NH_2^+ and OH_2^+ . For these data, the deflections are chosen so that the ESA detects only those protons with the maximum transverse momentum. The double coincidence rate for OH_2^+ peaks a little past the center of the proton cone—again consistent with a bond angle of 110° . However, for the other two projectiles, the peak occurs at the extreme angle of the proton cone—opposite the ESA. This would be consistent with a linear structure, but again vibrational effects may be playing a large role in these projectiles.

This work was performed under the auspices of the Division of Basic Energy Sciences of D.O.E.

References

1. E. P. Kanter, *this conference*.
2. Z. Vager and D. S. Gemmell, *Phys. Rev. Lett.* **37**, 1352 (1976).
3. D. S. Gemmell, *Radiation Research* (Proc. of the Sixth Int. Congress of Radiation Research, Tokyo, Japan, 13-19 May 1979), ed. by S. Okada, M. Imamura, T. Terashima and H. Yamaguchi (U. of Tokyo, 1979), pp. 132-144.
4. E. P. Kanter, P. J. Cooney, D. S. Gemmell, K.-O. Groeneveld, W. J. Pietsch, A. J. Ratkowski, Z. Vager and B. J. Zabransky, *Phys. Rev.* **A20**, 834 (1979).
5. D. S. Gemmell, *Nucl. Instrum. Methods* **170**, 41 (1980).

6. M. J. Gaillard, D. S. Gemmell, G. Goldring, I. Levine, W. J. Pietsch, J.-C. Poizat, A. J. Ratkowski, J. Remillieux, Z. Vager and B. J. Zabransky, *Phys. Rev.* **A17**, 1797 (1978).
7. D. S. Gemmell, E. P. Kanter and W. J. Pietsch, *Chem. Phys. Lett.* **55**, 331 (1978).
8. D. S. Gemmell, *Chemical Reviews* (Aug. 1980), in press.
9. D. S. Gemmell, P. J. Cooney and E. P. Kanter, *Nucl. Instrum. Methods* **170**, 81 (1980).
10. D. S. Gemmell, E. P. Kanter and W. J. Pietsch, *J. Chem. Phys.* **72**, 6818 (1980).
11. Proceedings of the Workshop on Physics with Fast Molecular-Ion Beams, Argonne National Laboratory, Argonne, IL., 20-21 August 1979, ed. by D. S. Gemmell, Physics Division Informal Report ANL/PHY-79-3 (August 1979).
12. A. Breskin, A. Faibis, G. Goldring, M. Hass, R. Kaim, I. Plessner, Z. Vager and N. Zwang, p. 1 of Ref. 11.
13. G. Goldring, Y. Eisen, P. Thieberger and H. Wegner, p. 27 of Ref. 11.
14. G. D. Carney, *Molec. Phys.* **39**, 923 (1980).
15. D. L. Smith and J. H. Futrell, *J. Phys. B*, **8**, 803 (1975).
16. G. Herzberg, *Electronic spectra of polyatomic molecules* (Van Nostrand, Princeton 1950).
17. R. N. Dixon, *Molec. Phys.* **20**, 113 (1971).
18. N. Cue, A. K. Edwards, D. S. Gemmell, I. Plessner and J.-C. Poizat (to be published).
19. N. Cue, A. K. Edwards, D. S. Gemmell, E. P. Kanter, I. Plessner, and J.-C. Poizat (to be published).
20. H. Lew and I. Heiber, *J. Chem. Phys.* **58**, 1246 (1973); H. Lew, *Can. J. Phys.* **54**, 2028 (1976).

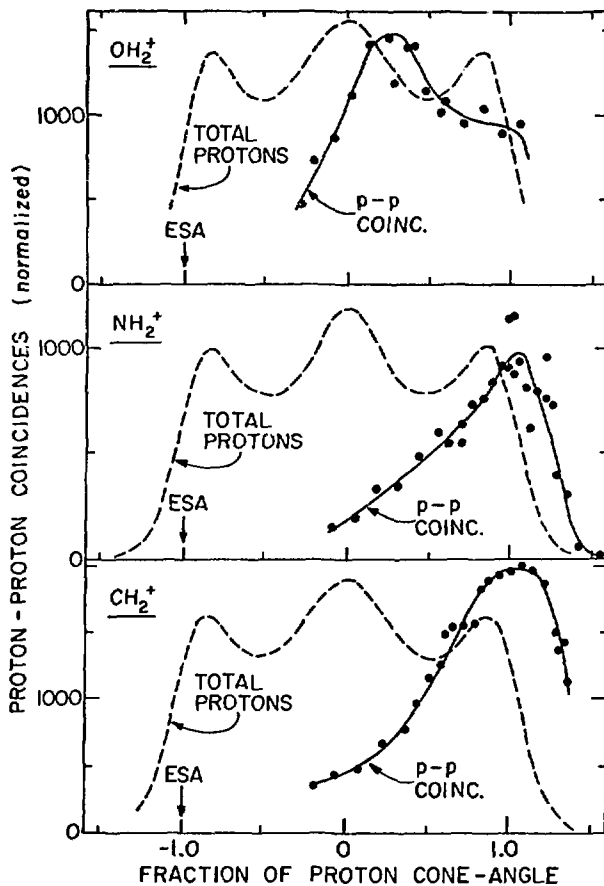


Fig. 9. The proton-proton coincidence counting rates for 3.6-MeV beams of CH_2^+ , NH_2^+ and OH_2^+ dissociating in carbon foils of thicknesses 98 Å, 66 Å and 89 Å, respectively (Ref. 9). The rates are plotted as functions of the fraction of the proton cone angle (16.25, 14.28 and 13.21 mrad for CH_2^+ , NH_2^+ and OH_2^+ , respectively) lying between the electrostatic analyzer (set on the protons having the maximum transverse momentum) and one of the movable surface barrier detectors (Fig. 6). Also shown are the total (energy-summed) proton-singles rates in the movable detector.